

Inverted hysteresis loops observed in a randomly distributed cobalt nanoparticle system

JungYup Yang, JooHyung Kim, JunSeok Lee, SeokJong Woo, JuneSik Kwak, and JinPyo Hong*

New Functional Materials and Devices Laboratory, Department of Physics, Hanyang University, Seoul 133-791, Republic of Korea

MyungHwa Jung

Quantum Material Research Team, Korean Basic Science Institute, Daejeon 305-333, Republic of Korea

(Received 31 January 2008; revised manuscript received 1 August 2008; published 17 September 2008)

We observed abnormal magnetic behaviors (so-called inverted hysteresis loops or negative remanence) in a randomly distributed Co nanoparticle (NP) system, where the Co NPs are prepared using laser irradiation. The inverted hysteresis loops are observed when ferromagnetic and superparamagnetic phases coexist within the NP system. Normal hysteresis loops appear in samples having only one phase, either ferromagnetic or superparamagnetic. The ferromagnetic and superparamagnetic Co NPs, with average diameters of 25 and 4 nm, respectively, showed negative remanence over a temperature range of 92–300 K. We have proposed that these abnormal features are directly related to the dipolar interaction between the superparamagnetic Co NPs and a ferromagnetic Co NP.

DOI: [10.1103/PhysRevB.78.094415](https://doi.org/10.1103/PhysRevB.78.094415)

PACS number(s): 75.75.+a, 75.60.-d, 76.60.Es, 75.50.Tt

I. INTRODUCTION

Nanometer scale materials have recently attracted attention for possessing interesting magnetic, transport, and mechanical properties, depending on the size distribution of the particles.¹⁻³ Magnetic nanometer-scale materials [so-called magnetic nanoparticles (NPs)] have drawn particular interest and are the subject of a broad range of investigations in physics, chemistry, biology, and materials science. Due to their small size, magnetic NPs exhibit novel material properties that differ considerably from those in the bulk solid state.⁴⁻⁶ In this emerging field, fine magnetic nanoparticles are desirable owing to their broad range of applications, especially in data storage devices, and biosensors, among others.⁷⁻⁹

Hysteresis loops are important phenomena observed in materials that are nearly magnetic, and they reflect the properties of the material.¹⁰ Generally, the behavior of the loop is governed not only by intrinsic properties of the material but also by extrinsic factors such as temperature, shape, and interaction, for example. In addition, a common characteristic of the hysteresis loop is that the magnetization does not decrease to zero but remains positive when the field decreases from positive saturation to zero.¹¹ The abnormal magnetic behavior of ferromagnetic (FM) materials was first challenged by Esho in 1976.¹² It was found that the hysteresis loops for amorphous Gd-Co films showed a negative remanence and inverted hysteresis loop behavior. This means that the hysteresis loops progress in a clockwise direction, displaying a negative remanence and coercivity. This anomalous hysteresis behavior was not only found in this particular system; it was also observed in many other systems.¹³⁻¹⁶ For example, O'Shea *et al.*¹³ presented a two-phase theory for inhomogeneous systems (ferromagnetic-antiferromagnetic systems) in which a highly anisotropic phase with a small magnetic moment is antiferromagnetically coupled to a phase with a small amount of anisotropy and a large magnetic moment.¹⁴ Geshev *et al.*¹⁵ built on this theory by extending it to systems involving competing cubic and uniaxial anisotropy, as well as to systems with two competing

uniaxial anisotropies. Some authors argued that the magnetostatic interaction between different parts of the inhomogeneous system was responsible for the inverted hysteresis.¹⁶ Although a large number of studies have investigated inverted hysteresis loops, clear explanation of inverted hysteresis loops in magnetic NP systems has not yet been presented.

In this study, we present the inverted magnetic hysteresis loops of a randomly distributed Co NP system, where the Co NPs are prepared using laser irradiation. We believe that there are both superparamagnetic (SP) and ferromagnetic Co NP phases in our system, a conclusion supported by surface transmission electron microscopy (TEM). A theoretical interpretation based on the Stoner-Wohlfarth model¹⁷ was performed in order to explain possible causes of the inverted hysteresis loops.

II. EXPERIMENTS

The Co NPs were prepared on Si substrates by applying external laser irradiation to ultrathin Co films (nanometer scale thickness) at room temperature. The Co thin films were deposited using an ultrahigh-vacuum sputtering instrument at a base pressure of 10^{-8} Torr. The light source utilized during experimentation was a 355 nm wavelength Nd doped yttrium aluminum garnet (YAG) laser with a power of 2 W. The laser was focused on the sample through a focusing objective with a 0.5 mm round spot. The laser irradiation process and the fabrication of the NPs are described in more detail elsewhere.¹⁸ The formation of the NPs is stimulated by the surface strain effect induced by the rapid melting of the ultrathin Co film by laser irradiation. The structural properties of the Co NPs were studied in TEM images. Magnetic properties were measured from 5 to 300 K for all of the samples using a Quantum Design's superconducting quantum interference magnetometer (SQUID) magnetic properties measurement system (MPMS) system. The magnetic field was applied parallel to the plane of the samples in all measurements.

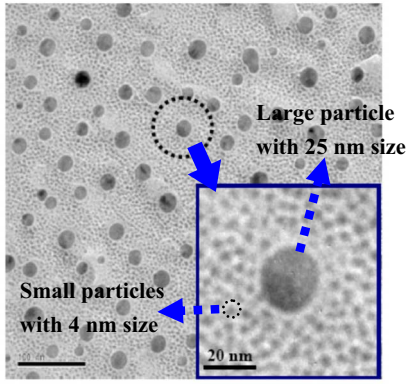


FIG. 1. (Color online) Typical plain-view TEM images of the Co NP system after laser irradiation at a laser power of 0.08 W and two scans. Inset figure shows an enlarged image of the area within the dotted circle line.

III. RESULTS AND DISCUSSIONS

Figure 1 shows a high-resolution TEM image of the Co NP system. As shown in Fig. 1, a large Co NP is surrounded by numerous relatively small Co NPs. The average diameters of the large and small Co NPs are 25 and 4 nm, respectively. The laser power used to generate these NPs was 0.08 W. The film was scanned by the laser twice. An inset figure shows an enlarged image of the area within the dotted circle. As shown in this inset, the size distribution of the Co NPs allows the NP system to have a ferromagnetic phase and a superparamagnetic phase simultaneously when in a specific temperature range.

Figure 2 shows the remanent magnetization (M_r) of the aforementioned sample as a function of temperature. The M_r was measured at each temperature upon the removal of the positive magnetic field from 3000 to 0 Oe. The positive magnetic field of 3000 Oe is essentially temperature independent, indicating that at this level, the magnetization is saturated. When the sample was cooled to 5 K (where the rotation of the particles was frozen), the measured M_r was a positive value. This behavior is similar to that of conventional ferromagnetic materials. Upon increasing the temperature, the M_r started to change sign, passing 0 at about 92 K. The measured M_r at 130 K is as large as -58% compared to the M_r value at 5 K. The zero M_r value at 92 K clearly suggests that there are Co NPs whose magnetization can follow the behavior of superparamagnetic material under an external magnetic field. Generally, the M_r of superparamagnetic NPs is zero because thermal fluctuations prevent the existence of stable magnetization. In our system, the observed zero M_r value at 92 K demonstrates that the moments are partially blocked below 92 K. At the temperatures where the M_r is negative, most of the small Co NPs become superparamagnetic. However, some large Co NPs can still maintain the ferromagnetic phase, as shown in the TEM image. The moment of the ferromagnetic Co NP affects the moments of the superparamagnetic Co NPs. This effect is due to the antiferromagnetically dipolar interaction between the two different sized particles. The total magnetic moment of the superparamagnetic Co NPs may be larger than that of one ferromag-

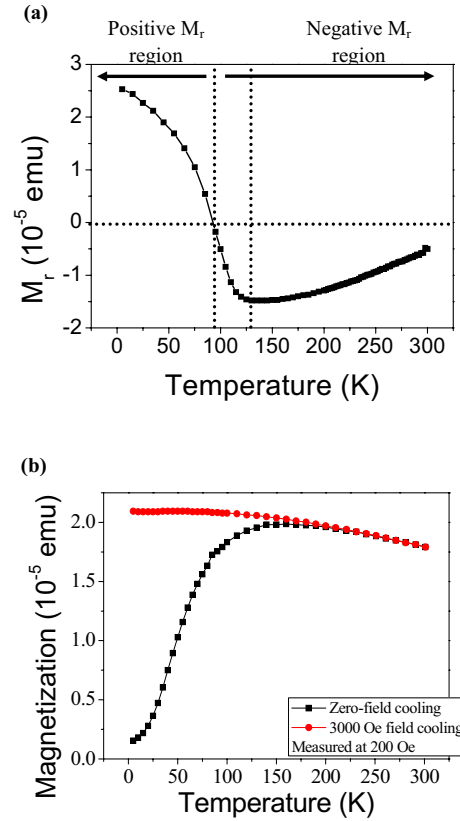


FIG. 2. (Color online) (a) Remanent magnetization as a function of temperature as measured by MPMS and (b) ZFC/FC curves of our Co NP system measured at 200 Oe.

netic Co NP if there is a sufficient population difference between the large and small particles. We suggest that the negative remanence must be considered in light of the interaction between the two different phases: that is, a ferromagnetic Co NP and superparamagnetic Co NPs.

The zero-field cooling (ZFC)/field cooling (FC) curve of our Co NP system is shown in Fig. 2(b). The temperature (T) dependence of the magnetic moment (emu) under an applied magnetic field of 200 Oe was measured after FC and after ZFC. As shown in this figure, the T_B is 150 K and the broad ZFC curve was presented. This broad ZFC curve indicates that the size of Co NPs is different in distribution because the FM Co NPs and the SP Co NPs appear at a mixture state on surface.

Figure 3 shows the hysteresis loops from 3000 to -3000 Oe and back to 3000 Oe measured at different temperatures. A normal magnetic hysteresis loop was obtained at 5 K, and the amplitude of the magnetic remanence is similar to the value in Fig. 2, as shown in Fig. 3(a). However, the M_r became negative at $T > 125$ K, as shown in Figs. 3(b) and 3(c). As indicated by the arrows, when the magnetic field (H) is reduced from saturation with positive values, the magnetization sign is reversed as a result of the positive coercive field, yielding a negative value ($M_r < 0$) for $H=0$. The reciprocal dependence is measured when the field is increased from negative saturation to a positive value. In addition, the value of negative remanence at 125 K is as large as 60% when it is compared to the positive saturated value, as shown

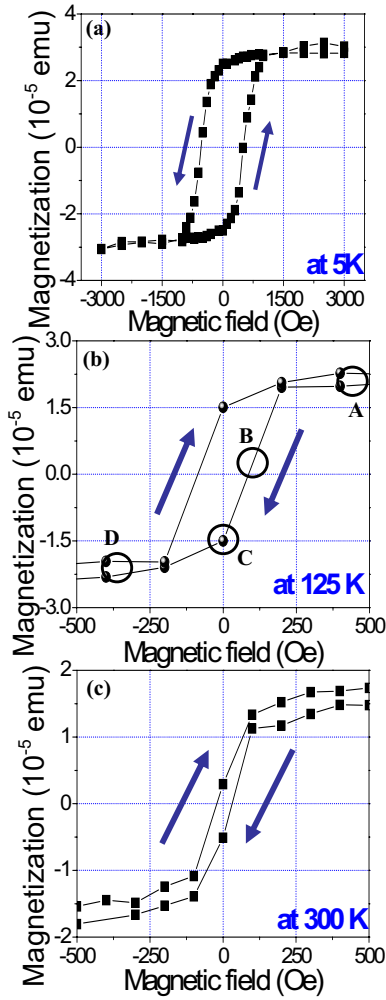


FIG. 3. (Color online) Magnetic hysteresis loops measured at (a) 5 K, (b) 125 K, and (c) 300 K. The direction of magnetic-field sweep is indicated by arrows. The A, B, C, and D marks in (b) are described in the text.

in Fig. 3(b). The hysteresis loops are inverted at temperatures greater than 125 K, as expected from the M_r - T curve. It should be noted that the inverted hysteresis loops are clockwise, in contrast to normal hysteresis loops that are counterclockwise. The A, B, C, and D marks in Fig. 3(b) are well described below.

Figure 4 shows the (a) surface analysis and (b) structural properties measured by the x-ray photoemission spectroscopy (XPS) and TEM electron-diffraction patterns, respectively. As shown in Fig. 4, the observation of XPS and TEM diffraction patterns presents the formation of CoO peak at the surface of Co NPs. It is natively formed by the surface oxidation process. Generally, it is known that the CoO is an antiferromagnetic material below 290 K. As mentioned in Sec. I, the ferromagnetic-antiferromagnetic coupled system makes possible inverted magnetic hysteresis loops due to the antiferromagnetically interaction between them. However, any shift in the magnetic hysteresis loops was not observed, as shown in Fig. 3. Therefore, although the CoO phase at the surface of Co NPs slightly affects the magnetization, it is not a dominant cause of inverted magnetic hysteresis loops.

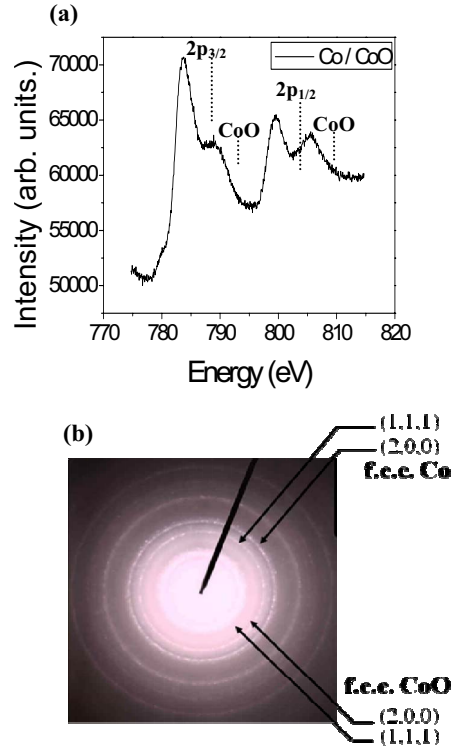


FIG. 4. (Color online) Structural properties of our Co NP system. (a) XPS result of Co $2p$ spectra of our Co NP system and (b) selective electron-diffraction pattern of our sample measured by the TEM system.

To better explain the inverted hysteresis loops in our Co NP system, we made the following four assumptions. First, the magnetization contribution of the two different magnetic phases arises from the ferromagnetic Co NP [large size nanoparticle (LSNP)] and the superparamagnetic Co NP [small size nanoparticle (SSNP)]. Second, the total magnetization (M_1) of the SSNPs around the LSNP is larger than that of one LSNP magnetization (M_2). Third, there is a large amount of magnetic anisotropy acting on the LSNP magnetization. Finally, there is no interaction between the LSNPs because of the long distance between them. According to the Stoner-Wohlfarth model¹⁷ with uniaxial anisotropy, the total energy of the system is given by

$$E = -M_1 V_1 H \cos(\theta_1 - \theta_H) - M_2 V_2 H \cos(\theta_2 - \theta_H) + K_1 V_1 \sin^2 \theta_1 + K_2 V_2 \sin^2 \theta_2 - J M_1 M_2 \cos(\theta_1 - \theta_2), \quad (1)$$

where K , V , and M are the anisotropy constants, volume, and saturation magnetization of each NP type, SSNP, and LSNP, respectively. H is the magnitude of the applied field. θ_1 and θ_2 are the angles of M_1 and M_2 with respect to the easy axis of magnetization of the SSNP and LSNP. θ_H is the angle between the easy axis of magnetization and the applied magnetic field. We assume in the calculation that the applied field is always kept along the easy axis direction ($\theta_H=0$). The first two terms represent the Zeeman contributions of the Co NPs (SSNP and LSNP). The next two terms represent the anisotropy energies of the Co NPs. The last term is the magnetic interaction energy between the LSNP and the SSNP.

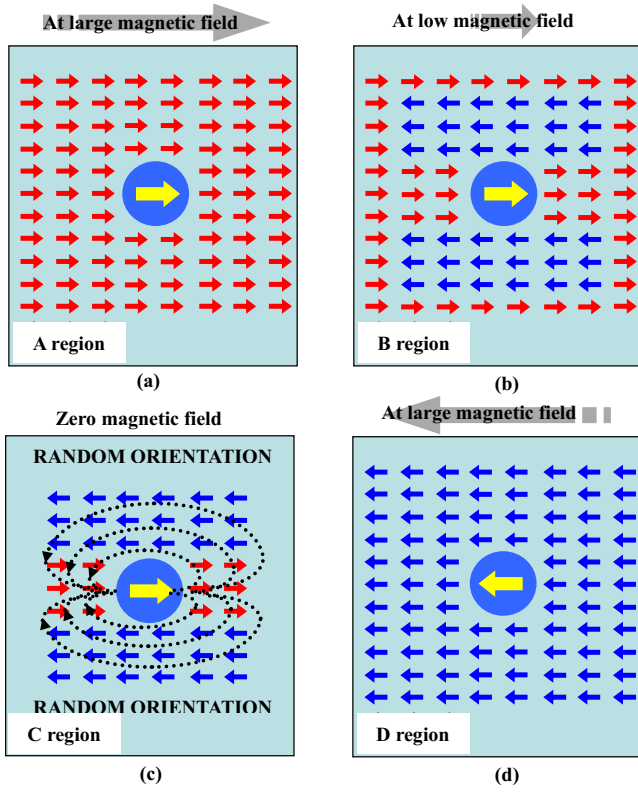


FIG. 5. (Color online) Schematic diagrams of the magnetization process with four different applied external magnetic fields: (a) large positive, (b) small positive, (c) zero, and (d) large negative external magnetic field.

First, we will explain the magnetization process of the whole system in three different temperature ranges: low temperature ($T < T_{\text{low}}$), intermediate temperature ($T_{\text{low}} < T < T_{\text{high}}$), and high temperature ($T > T_{\text{high}}$). The T_{low} and T_{high} indicate the below and above average blocking temperatures of the whole system. At low and high temperatures, the magnetization processes of the whole system present conventional ferromagnetic and superparamagnetic behaviors, respectively. The magnetization process of the whole system in the intermediate temperature region can be explained in four different cases depending on the applied magnetic field.

For the minimization of the system energy, $\partial E / \partial \theta_1$ and $\partial E / \partial \theta_2$ must be zero in expression.¹ The calculated solutions were four cases: (1) $\theta_1 = \theta_2 = 0$, (2) $\theta_1 = \pi$, $\theta_2 = 0$, (3) $\theta_1 = 0$, $\theta_2 = \pi$, and (4) $\theta_1 = \theta_2 = \pi$. The inverted hysteresis loops of our samples can be understood as follows, with the assistance of the schematic diagrams shown in Fig. 5. When a high external magnetic field is applied [Fig. 5(a)], the magnetization vectors of the LSNP and the SSNPs are lined up along the applied field direction in order to achieve a stable state ($\theta_1 = \theta_2 = 0$). This is marked as region A in Fig. 5(b). When the external magnetic field is decreased, as shown in region B in Fig. 5(b), the total magnetization value starts to decrease and spin rearrangement occurs in the SSNPs nearby the LSNP due to the antiferromagnetically magnetic interaction. In order to obtain the most stable state, the magnetization of the LSNP should be reversed, so as to minimize the total energy ($\theta_1 = 0$, $\theta_2 = \pi$). However, the magnetization of

the LSNP cannot be easily rotated due to the large amount of magnetic anisotropy present. As a result, the SSNP moments are rearranged in localized regions. Moreover, because of the presence of the LSNP, the SSNPs in the vicinity of the LSNP will be antiferromagnetically coupled against the magnetization direction of the LSNP in order to lower the total energy of the system [Fig. 5(b)].

When the external magnetic field becomes zero, the magnetic-moment direction of the SSNPs that are located far from the LSNP should follow the behavior of general superparamagnetism. Therefore, the SSNPs that are a long distance from the LSNP should be randomly orientated. The magnetization of the LSNP cannot be reversed due to the large magnetic anisotropy; however, the SSNPs will be antiferromagnetically coupled against the direction of the LSNP moment [Fig. 5(c)]. Significantly, the total magnetization value becomes more negative because the M_1 of the SSNPs is larger than the M_2 of the LSNP (second assumption mentioned above) as marked in region C of Fig. 5(b).

The magnetization state of $\theta_1 = \pi$, $\theta_2 = 0$ is maintained until the applied negative magnetic field reaches the anisotropic field of the LSNP. Then, since the external magnetic field is decreased, the magnetic moment of the LSNP can switch due to the large magnetic anisotropy, as shown in Fig. 5(d). The reciprocal dependence is observed when the field is increased from negative saturation to a positive value. Hence, we expect that the inverted hysteresis loops may be due to the magnetic dipolar interaction between ferromagnetic and superparamagnetic phases.

The results of our theoretic analysis based on the Stoner-Wohlfarth particle model¹⁷ differed slightly from the experimental results of our Co NP system. This difference is explained by the fact that the magnetic properties of the system depend on various features, such as surface state, shape, distribution, and texture, which are only present in the real system.

IV. CONCLUSION

We observed inverted magnetic hysteresis loops in our Co NP system consisting of large and small Co NPs. The Co NPs were uniquely fabricated using a laser irradiation technique. Magnetization measurements of the Co NP system exhibited negative remanence in the temperature range of 92–300 K. The observed negative remanence correlates to the presence of superparamagnetism in the small particles. Although we cannot present any clear theoretical simulation for the inverted magnetic hysteresis loops at this time, we suspect that this behavior is associated with the characteristics of the antiferromagnetically dipolar interaction between the ferromagnetic Co NP and the superparamagnetic Co NPs. Further investigation of the inverted magnetic hysteresis loops is currently being conducted using a commercially available micromagnetic simulation package.

ACKNOWLEDGMENTS

This work was supported by the Korea Research Foundation Grant funded by the Korean Government (Grant No. KRF-2007-313-C00243).

*jphong@hanyang.ac.kr

- ¹A. N. Dobrynin, D. N. Ievlev, K. Temst, P. Lievens, J. Margueritat, J. Gonzalo, C. N. Afonso, S. Q. Zhou, A. Vantomme, E. Piscopiello, and G. Van Tendeloo, *Appl. Phys. Lett.* **87**, 012501 (2005).
- ²S. Rusponi, N. Weiss, T. Cren, M. Epple, and H. Brune, *Appl. Phys. Lett.* **87**, 162514 (2005).
- ³J. Y. Cheng, C. A. Ross, E. L. Thomas, H. I. Smith, R. G. H. Lammertink, and G. J. Vancso, *IEEE Trans. Magn.* **38**, 2541 (2002).
- ⁴G. Schmid, *Nanoparticles: From Theory to Application* (Wiley, Weinheim, 2004).
- ⁵N. Singh, S. Goolaup, W. Tan, A. O. Adeyeye, and N. Balasubramaniam, *Phys. Rev. B* **75**, 104407 (2007).
- ⁶G. A. Held, G. Grinstein, H. Doyle, Shouheng Sun, and C. B. Murray, *Phys. Rev. B* **64**, 012408 (2001).
- ⁷L. Gunther, *Phys. World* **2**, 28 (1990).
- ⁸R. D. Shull, *IEEE Trans. Magn.* **29**, 2614 (1993).
- ⁹R. F. Ziolo, E. P. Giannelis, B. Weinstein, M. P. O'Horo, B. N. Ganguly, V. Mehrotra, M. W. Russell, and D. R. Huffman, *Science* **257**, 219 (1992).
- ¹⁰G. Bertotti, *Hysteresis in Magnetism* (Academic, New York, 1997).
- ¹¹S. Chikazumi, *Physics of Ferromagnetism* (Oxford University Press, New York, 1997).
- ¹²S. Esho, *Jpn. J. Appl. Phys., Suppl.* **15**, 93 (1976).
- ¹³M. J. O'Shea, H. Jiang, P. Perera, and H. H. Hamdeh, *J. Appl. Phys.* **87**, 6137 (2000).
- ¹⁴Y. Z. Wu, G. S. Dong, and X. F. Jin, *Phys. Rev. B* **64**, 214406 (2001).
- ¹⁵J. Geshev, A. D. C. Viegas, and J. E. Schmidt, *J. Appl. Phys.* **84**, 1488 (1998).
- ¹⁶X. Yan and Y. Xu, *J. Appl. Phys.* **79**, 6013 (1996).
- ¹⁷E. C. Stoner and E. P. Wohlfarth, *Philos. Trans. R. Soc. London, Ser. A* **240**, 599 (1948).
- ¹⁸J. Y. Yang, K. S. Yoon, Y. H. Do, C. O. Kim, J. P. Hong, Y. H. Rho, and H. J. Kim, *J. Appl. Phys.* **93**, 8766 (2003).